

Einstein–de Haas Effect in Dipolar Bose-Einstein Condensates

Yuki Kawaguchi,¹ Hiroki Saito,¹ and Masahito Ueda^{1,2}

¹*Department of Physics, Tokyo Institute of Technology, 2-12-1 Ookayama, Meguro-ku, Tokyo 152-8551, Japan*

²*ERATO, Japan Science and Technology Corporation (JST), Saitama 332-0012, Japan*

(Received 2 November 2005; published 3 March 2006)

The general properties of the order parameter for a dipolar spinor Bose-Einstein condensate are discussed based on symmetries of interactions. An initially spin-polarized dipolar condensate is shown to dynamically generate a nonsingular vortex via spin-orbit interactions—a phenomenon reminiscent of the Einstein–de Haas effect in ferromagnets.

DOI: [10.1103/PhysRevLett.96.080405](https://doi.org/10.1103/PhysRevLett.96.080405)

PACS numbers: 03.75.Mn, 03.75.Kk, 03.75.Lm, 03.75.Nt

The realization of a Bose-Einstein condensate (BEC) of ^{52}Cr [1,2] marks a major development in degenerate quantum gases in that the interparticle interaction via magnetic dipoles in this BEC is much larger than those in other spinor BECs of alkali atoms. The long-range nature and anisotropy of the dipolar interaction poses challenging questions concerning the stability and superfluidity of the BEC [3–10]. The ground state of the ^{52}Cr atom has a total electronic spin of three and a nuclear spin of zero, and therefore the ^{52}Cr BEC has seven internal degrees of freedom. The interplay between dipolar and spinor interactions makes the order parameter of this system highly nontrivial [11–13]. Moreover, the dipole interaction couples the spin and orbital angular momenta so that an initial magnetization of the system causes the gas to rotate mechanically (Einstein–de Haas effect [14]) or, conversely, solid-body rotation of the system leads to its magnetization (Barnett effect [15]).

This Letter investigates the Einstein–de Haas and Barnett effects in a spin-3 BEC system. We discuss the symmetry of the order parameter of a dipolar spinor BEC and study the dynamic formation of spin textures using numerical simulations of the seven-component nonlocal mean-field theory, which takes into account short-range (van der Waals) interactions and magnetic dipole-dipole interactions subject to a trapping potential and an external magnetic field.

We first consider the general properties of the order parameter by discussing two fundamental symmetries of the dipolar interaction between the magnetic dipole moments $\boldsymbol{\mu}_1 = g\mu_B\hat{s}_1$ and $\boldsymbol{\mu}_2 = g\mu_B\hat{s}_2$, where g is the electron g factor, μ_B is the Bohr magneton, and \hat{s}_1 and \hat{s}_2 are the spin operators. The interaction between the magnetic dipoles located at \mathbf{r}_1 and \mathbf{r}_2 is described by

$$\hat{v}_{\text{dd}}(\mathbf{r}_{12}) = c_{\text{dd}} \frac{(\hat{s}_1 \cdot \hat{s}_2) - 3(\hat{s}_1 \cdot \mathbf{e}_{12})(\hat{s}_2 \cdot \mathbf{e}_{12})}{r_{12}^3}, \quad (1)$$

where $\mathbf{r}_{12} \equiv \mathbf{r}_1 - \mathbf{r}_2$, $\mathbf{e}_{12} \equiv \mathbf{r}_{12}/r_{12}$, and $c_{\text{dd}} = \mu_0(g\mu_B)^2/4\pi$, with μ_0 being the magnetic permeability of the vacuum. The dipole interaction is invariant under simultaneous rotation in spin and coordinate spaces about

an arbitrary axis, say the z axis, so that the projected total angular momentum operator $\hat{S}_z + \hat{L}_z$ on that axis commutes with \hat{v}_{dd} , where $\hat{S} = \hat{s}_1 + \hat{s}_2$ is the total spin operator and \hat{L} is the relative orbital angular momentum operator. Another symmetry of the dipolar interaction is the invariance under the transformation $\mathbf{P}_z e^{-i\pi\hat{S}_z}$, where $\mathbf{P}_z: (x, y, z) \rightarrow (x, y, -z)$ and $e^{-i\pi\hat{S}_z}: (\hat{S}_x, \hat{S}_y, \hat{S}_z) \rightarrow (-\hat{S}_x, -\hat{S}_y, \hat{S}_z)$. Thus, the eigenvalues of the following operators are conserved by the dipole interaction:

$$\hat{S}_z + \hat{L}_z \quad \text{and} \quad \mathbf{P}_z e^{-i\pi\hat{S}_z}. \quad (2)$$

A crucial observation is that these operators also commute with the short-range interactions. Thus, if the confining potential is axisymmetric, the simultaneous eigenfunctions of the two operators (2) can serve to classify the two-body wave function.

Constructing a many-body wave function by directly applying these symmetry considerations is quite complicated since the system has many degrees of freedom. However, substantial simplification can be achieved by considering the case of a ferromagnet in which dipole moments are localized at lattice sites and thus the degrees of freedom of the system are reduced to the center-of-mass motion and the solid-body rotation around it. Consequently, spin relaxation of the system leads to a solid-body rotation of the ferromagnet—the Einstein–de Haas effect [14]. An analogous consideration can be applied to a BEC because almost all atoms occupy a single-particle state and therefore the degrees of freedom of the system can be represented by those of the order parameter. We may thus expect the Einstein–de Haas effect to emerge in a dipolar spinor BEC system.

In general, the order parameter of a BEC can be defined as the eigenfunction corresponding to the macroscopic eigenvalue of the reduced single-particle density operator. Let the order parameter be denoted as $\psi_\alpha(\mathbf{r})$ with a norm assumed to be N , the number of condensate atoms. Here, α represents the magnetic sublevels of the atoms. It follows from the above symmetry considerations of the dipolar interaction that the order parameter of a dipolar spinor

BEC in an axisymmetric system can be classified by the eigenvalues of the operators $\hat{s}^z + \hat{l}^z$ and $\mathbf{P}_z \exp(-i\pi\hat{s}^z)$ corresponding to the operators (2), where \hat{s}^z is the z component of the spin matrix and $\hat{l}^z \equiv -i(\partial/\partial\phi)$. The simultaneous eigenstate of $\hat{s}^z + \hat{l}^z$ and $\mathbf{P}_z \exp(-i\pi\hat{s}^z)$ with eigenvalues J and p , respectively, is given by

$$\psi_\alpha(r, \phi, z, t) = e^{i(J-\alpha)\phi} \eta_{\alpha J p}(r, z, t), \quad (3)$$

where J is an integer and $\eta_{\alpha J p}$ is a complex eigenfunction of \mathbf{P}_z satisfying $\mathbf{P}_z \eta_{\alpha J p} = p(-1)^\alpha \eta_{\alpha J p}$ with $p = \pm 1$. A key point of Eq. (3) is that it includes the spin-dependent phase factor, since the dipolar interaction couples the spin with the orbital angular momentum.

We now consider the dynamic formation of spin textures in a dipolar BEC. The order parameter obeys the following set of the nonlocal Gross-Pitaevskii equations:

$$\begin{aligned} i\hbar \frac{d\psi_\alpha(\mathbf{r})}{dt} = & \left[-\frac{\hbar^2 \nabla^2}{2M} + g\mu_B B_{\text{ext}} \alpha + U_{\text{trap}}(\mathbf{r}) \right] \psi_\alpha(\mathbf{r}) \\ & + \sum_{\beta\alpha'\beta'} \sum_{S=0}^{2s} g_S \langle \alpha\beta | \mathcal{P}_S | \alpha'\beta' \rangle \psi_{\beta'}^*(\mathbf{r}) \psi_{\alpha'}(\mathbf{r}) \psi_{\beta'}(\mathbf{r}) \\ & + \sum_{\mu=x,y,z} \sum_{\beta} B_{\text{eff}}^\mu(\mathbf{r}) (g\mu_B s_{\alpha\beta}^\mu) \psi_\beta(\mathbf{r}), \end{aligned} \quad (4)$$

where M is the atomic mass, B_{ext} is the external magnetic field in the z direction, and $U_{\text{trap}}(\mathbf{r})$ is the trapping potential. We assume an optical trap so that all spin components experience the same trapping potential. The second line in Eq. (4) represents the short-range interaction, where the strength of the interaction is characterized by the s -wave scattering length a_S for a total spin S of a pair of atoms with spin s as $g_S = 4\pi\hbar^2 a_S/M$. The operator \mathcal{P}_S projects the wave function into the Hilbert space with a total spin S and is represented in terms of the Clebsch-Gordan coefficients $\langle s\alpha s\beta | SM_S \rangle$ as $\langle \alpha\beta | \mathcal{P}_S | \alpha'\beta' \rangle = \sum_{M_S=-S}^S \langle s\alpha s\beta | SM_S \rangle \times \langle SM_S | s\alpha' s\beta' \rangle$ [16].

The last line in Eq. (4) represents the dipole-dipole interaction, where $s^{x,y,z}$ are the spin matrices, and

$$B_{\text{eff}}^\mu(\mathbf{r}) \equiv \frac{c_{\text{dd}}}{g\mu_B} \sum_{\nu} \int d\mathbf{r}' \frac{\delta_{\mu\nu} - 3e^\mu e^\nu}{|\mathbf{r} - \mathbf{r}'|^3} \sum_{\alpha'\beta'} \psi_{\alpha'}^*(\mathbf{r}') s_{\alpha'\beta'}^\nu \psi_{\beta'}(\mathbf{r}') \quad (5)$$

is the effective magnetic field at \mathbf{r} produced by the surrounding magnetic dipoles, with $\mathbf{e} \equiv (\mathbf{r} - \mathbf{r}')/|\mathbf{r} - \mathbf{r}'|$. Calculating the time derivative of $S^\mu(\mathbf{r}) = \sum_{\alpha\beta} \psi_\alpha^*(\mathbf{r}) s_{\alpha\beta}^\mu \psi_\beta(\mathbf{r})$, we find that, apart from the spinor interactions, $\mathbf{S}(\mathbf{r})$ behaves like a classical spin and undergoes Larmor precession around the effective local magnetic field $\mathbf{B}_{\text{eff}}(\mathbf{r}) + B_{\text{ext}}\hat{z}$. Hence, spin flip occurs in the region where $B_{\text{eff}}^x(\mathbf{r}) \neq 0$. In a homogeneous infinite system, the effective field is completely canceled in a polarized BEC and spin flip does not occur. Therefore, the

Einstein-de Haas effect in an initially fully spin-polarized BEC is unique to nonuniform systems.

We now examine the spin dynamics of the Einstein-de Haas effect in a spin-3 ^{52}Cr BEC system. We consider a stable spin-polarized BEC in the lowest magnetic sublevel $\alpha = -3$, produced in a strong magnetic field, as in the experiments of Refs. [1,2]. We then suddenly decrease the magnetic field to B_{ext} . The initial state can be calculated by the imaginary-time propagation method in the subspace of $\psi_{-3}(\mathbf{r})$. We have performed three-dimensional simulations of Eq. (4) with seven spin components by using the Crank-Nicolson method. The scattering lengths of ^{52}Cr are reported to be $a_6 = 112$, $a_4 = 58$, and $a_2 = -7$ in units of the Bohr radius [17]. The value of a_0 is unknown and we estimate it using the van der Waals coefficient C_6 given in Ref. [17], obtaining $a_0 \sim (C_6 M/m_e)^{1/4} = 91$, where m_e is the electron mass. Since we are interested in the spin dynamics from a fully spin-polarized state, the short-range interaction is dominated by a_6 and a_4 [18].

We assume $N = 10^5$ atoms trapped in an axisymmetric potential $U_{\text{trap}}(\mathbf{r}) = (1/2)M\omega^2(r^2 + z^2/\lambda^4)$ with $\omega = 2\pi \times 820$ Hz. The typical ratio of the dipolar interaction to the short-range interaction is $s^2 c_{\text{dd}}/g_6 \approx 0.03$ with $s = 3$. In a spherical trap, the number density at the trap center is $n \approx 7 \times 10^{20} \text{ m}^{-3}$ and the dipole-dipole interaction energy $s^2 c_{\text{dd}} n$ becomes of the same order of magnitude as the Zeeman energy for $B_{\text{ext}} \approx 0.1$ mG. Hence, the spin-flip rate becomes significant for $|B_{\text{ext}}| \lesssim 1$ mG. In the following, we first consider $B_{\text{ext}} = 0$ and $\lambda = 1$, and then discuss the effects of the external magnetic field and the trap geometry on the spin dynamics.

Figure 1 shows the results for $B_{\text{ext}} = 0$ and $\lambda = 1$. In Fig. 1(a), we plot the population of each spin state $N_\alpha/N \equiv \int d\mathbf{r} |\psi_\alpha|^2/N$ as a function of ωt . The figure shows that N_{-2}/N first increases rapidly and then the components with $\alpha \geq -1$ begin to increase. Figs. 1(b)–1(d) show three-dimensional plots of ψ_{-3} , ψ_{-2} , and ψ_{-1} , respectively, at $\omega t = 2$, where $|\psi_\alpha|^2$ is scaled by N/a_{ho}^3 with a_{ho} being the harmonic oscillator length $\sqrt{\hbar/2M\omega}$. The order parameters show the symmetries of Eq. (3): ψ_{-2} has a phase factor $e^{-i\phi}$ and a node plane at $z = 0$, and ψ_{-1} has a phase factor $e^{-2i\phi}$ and has reflection symmetry with respect to the $z = 0$ plane. The other spin components have double-ring shapes similar to that of Fig. 1(d) and their phase relationships satisfy Eq. (3) with $J = -3$ and $p = -1$. Beyond $\omega t = 5$, the spinor order parameter of the system develops a complicated structure.

The effective magnetic field, Eq. (5), at $\omega t = 0$ and the spin vector $\mathbf{S}(\mathbf{r})$ at $\omega t = 2$ are plotted in Fig. 2. The whirling patterns of the spin texture in Figs. 2(b) and 2(c) are due to Larmor precession around the local magnetic field, shown in Fig. 2(a). Since the local magnetic field points outward for $z > 0$ and inward for $z < 0$, the directions of the whirlpools in Figs. 2(b) and 2(c) are opposite. Topological spin textures in spinor BECs have

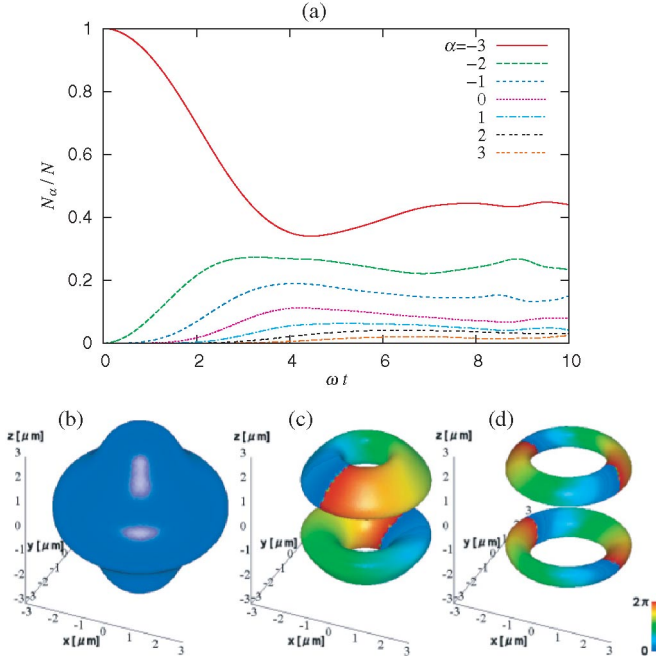


FIG. 1 (color). (a) Relative population $N_\alpha/N = \int dr |\psi_\alpha|^2/N$ of each magnetic sublevel α versus ωt for $B_{\text{ext}} = 0$ and $\lambda = 1$. (b)–(d) Isopycnic surfaces of (b) ψ_{-3} , (c) ψ_{-2} , and (d) ψ_{-1} at $\omega t = 2$, where $|\psi_\alpha|^2 a_{\text{ho}}^3/N = 0.0001$ for (b) and (c) and 5×10^{-5} for (d). The color on the surfaces represents the phase of the order parameter (refer to scale at right).

been observed in a spin-1/2 system [19] and in a spin-1 system [20]. We note that the spin textures in Figs. 2(b) and 2(c) are generated spontaneously due to the intrinsic dipole interaction, in contrast to those in Refs. [19,20], which are generated by external forces.

When the external magnetic field B_{ext} is applied in the positive z direction and is much stronger than the dipole field, the spin angular momentum should be conserved because of energy conservation and spin flipping is suppressed. When $B_{\text{ext}} < 0$, spin flip can occur by converting Zeeman energy to kinetic energy. These behaviors are demonstrated in Fig. 3(a), which shows the time evolution of N_{-2}/N for $B_{\text{ext}} = \pm 1$ mG. Figs. 3(b) and 3(c) show cross sections of $|\psi_{-2}|^2 a_{\text{ho}}^3/N$ for $B_{\text{ext}} = \pm 1$ mG at $\omega t = 8$ and $\lambda = 1$. When $B_{\text{ext}} > 0$, ψ_{-2} oscillates in time between the structures of Fig. 1(c) and Fig. 3(b). These structures derive from the symmetry of the dipole interaction, which can be expressed in terms of rank-2 spherical harmonics Y_{2m} . The dipole field produced by an approximately spherical distribution of $\psi_{-3} \sim Y_{00}(\mathbf{r})$ induces a $Y_{2-1}(\mathbf{r})$ term in ψ_{-2} [Fig. 1(c)], which in turn affects itself and induces a linear combination of $Y_{2-1}(\mathbf{r})$ and $Y_{4-1}(\mathbf{r})$, resulting in Fig. 3(b). Therefore, the structure in Fig. 3(b) manifests as a secondary effect of the dipole-dipole interaction. In the case of $B_{\text{ext}} = -1$ mG, a similar structure as in Fig. 3(b) appears for $\omega t \lesssim 4$. However, as time advances, the domain structure develops as shown in Fig. 3(c). The domain size becomes smaller as $|B_{\text{ext}}|$ increases.

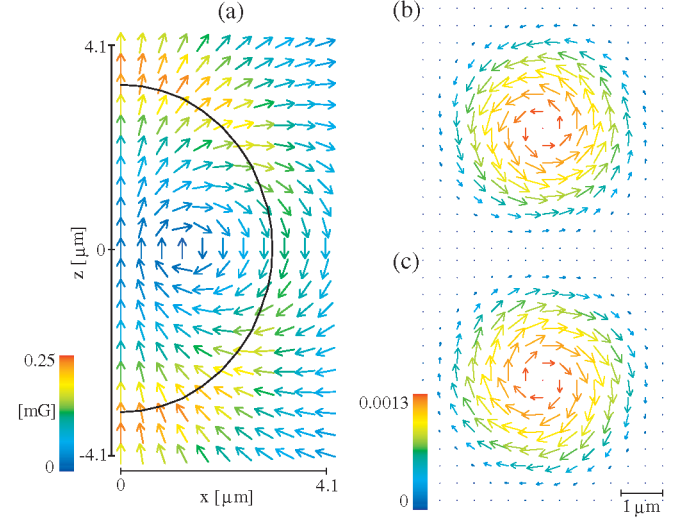


FIG. 2 (color). (a) Dipole field at $t = 0$ for $\lambda = 1$. The solid line shows the isopycnic curve at $|\psi_{-3}|^2 a_{\text{ho}}^3/N = 0.0001$. The color of the arrows denotes the magnitude of the field. (b),(c) Spin configurations on the (b) $z = 2 \mu\text{m}$ plane and (c) $z = -2 \mu\text{m}$ plane at $\omega t = 2$ for $B_{\text{ext}} = 0$ and $\lambda = 0$. The length of the arrows represents the magnitude of the spin vector projected on the xy plane and the color shows $|S|a_{\text{ho}}^3/N$. Note that the spins tilt in a direction perpendicular to $\mathbf{B}_{\text{eff}}(\mathbf{r})$.

Finally, we discuss the geometry dependence of the dynamics. Figure 4 shows the dipole field $\mathbf{B}_{\text{eff}}(\mathbf{r})$ at $t = 0$ for $\lambda = 0.5$. Compared with Fig. 2(a), the z component of the effective magnetic field is inverted around the center

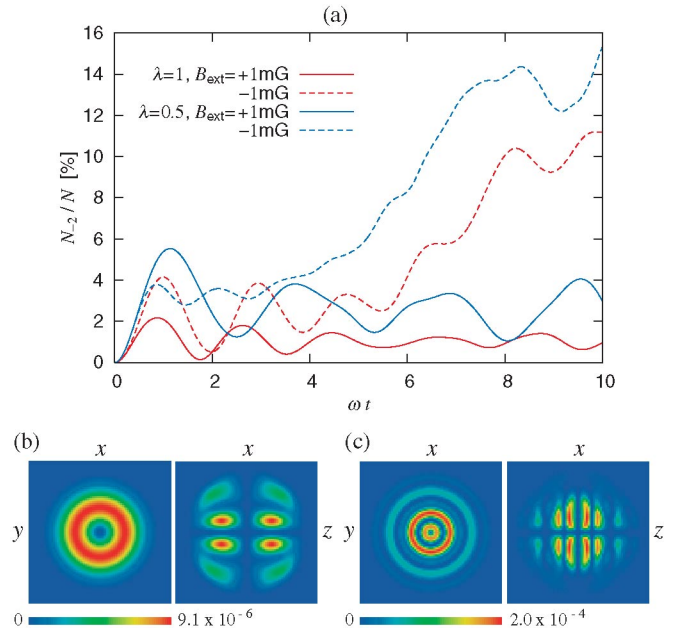


FIG. 3 (color). (a) Population of $\alpha = -2$ sublevel versus ωt for $B_{\text{ext}} = \pm 1$ mG and $\lambda = 1$ and 0.5 . (b),(c) Cross sections of $|\psi_{-2}|^2 a_{\text{ho}}^3/N$ with $\lambda = 1$ at $\omega t = 8$ for (b) $B_{\text{ext}} = 1$ mG and (c) $B_{\text{ext}} = -1$ mG. The cross sections are at $z = 0.7 \mu\text{m}$ (left) and $y = 0 \mu\text{m}$ (right). The size of each panel is $8.2 \times 8.2 \mu\text{m}$.

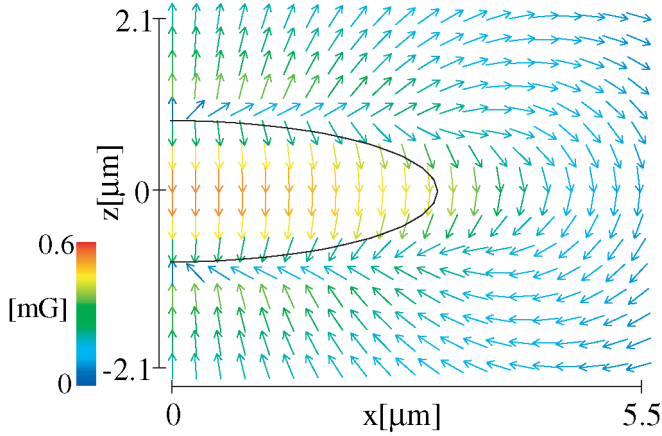


FIG. 4 (color). Dipole field at $t = 0$ for $\lambda = 0.5$. The solid line shows the isopycnic curve at $|\psi_{-3}|^2 a_{\text{ho}}^3 / N = 0.0005$. Note that the sign of $B_{\text{eff}}^z(\mathbf{r})$ in the condensate is opposite to that in Fig. 2(a).

of the condensate. The transfer of atoms from the spin component $\alpha = -3$ to $\alpha \geq -2$ is due to the Larmor precession caused by B_{eff}^{xy} , and it occurs most efficiently at the place where the local magnetic field in the z direction $B_{\text{eff}}^z + B_{\text{ext}}$ vanishes. The sign of such an optimized B_{ext} for spherical traps is opposite to that for pancake-shaped traps, as can be inferred from Figs. 2(a) and 4. This fact is reflected in Fig. 3(a) as the difference in the field dependence of the initial peaks. Since the z component of the dipole field is positive for most of the condensate when $\lambda = 1$ [Fig. 2(a)], the initial peak in Fig. 3(a) is larger for $B_{\text{ext}} = -1$ mG than for $B_{\text{ext}} = 1$ mG. The relation between the initial peak and B_{ext} is opposite for $\lambda = 0.5$, since the z component of the dipole field is mostly negative in the condensate (Fig. 4). In the case of a cigar-shaped BEC, the qualitative behavior is the same as for the spherical trap.

In conclusion, we have shown that the Einstein–de Haas effect occurs in dipolar spinor Bose-Einstein condensates and that a nonsingular vortex appears from an initially spin-polarized condensate. In a low magnetic field (~ 1 mG) the fraction of the spin-flipped atoms ($\sim 5\%$) is large enough to be observed in Stern-Gerlach experiments. The spin-relaxation processes produce various vortex structures, depending on the external magnetic field.

This work was supported by Grant-in-Aids for Scientific Research (Grants No. 17740263, No. 17071005, and No. 15340129) and by a 21st Century COE program at Tokyo Tech “Nanometer-Scale Quantum Physics” from the Ministry of Education, Culture, Sports, Science and Technology of Japan. Y.K. acknowledges the support of

the Japan Society for Promotion of Science (Project No. 160648). M.U. acknowledges support by a CREST program of the JST.

Note added.—Very recently, a preprint [21] has appeared which also discusses the Einstein–de Haas effect in a dipolar BEC.

-
- [1] A. Griesmaier, J. Werner, S. Hensler, J. Stuhler, and T. Pfau, Phys. Rev. Lett. **94**, 160401 (2005).
 - [2] J. Stuhler, A. Griesmaier, T. Koch, M. Fattori, T. Pfau, S. Giovanazzi, P. Pedri, and L. Santos, Phys. Rev. Lett. **95**, 150406 (2005).
 - [3] L. Santos, G. V. Shlyapnikov, P. Zoller, and M. Lewenstein, Phys. Rev. Lett. **85**, 1791 (2000).
 - [4] L. Santos, G. V. Shlyapnikov, and M. Lewenstein, Phys. Rev. Lett. **90**, 250403 (2003).
 - [5] K. Góral and L. Santos, Phys. Rev. A **66**, 023613 (2002).
 - [6] K. Góral, K. Rzazewski, and T. Pfau, Phys. Rev. A **61**, 051601(R) (2000).
 - [7] D.H.J. O’Dell, S. Giovanazzi, and C. Eberlein, Phys. Rev. Lett. **92**, 250401 (2004).
 - [8] C. Eberlein, S. Giovanazzi, and D.H.J. O’Dell, Phys. Rev. A **71**, 033618 (2005).
 - [9] S. Yi and L. You, Phys. Rev. A **63**, 053607 (2001).
 - [10] M. Baranov, L. Dobrek, K. Góral, L. Santos, and M. Lewenstein, Phys. Scr. **T102**, 74 (2002).
 - [11] S. Yi, L. You, and H. Pu, Phys. Rev. Lett. **93**, 040403 (2004).
 - [12] H. Pu, W. Zhang, and P. Meystre, Phys. Rev. Lett. **87**, 140405 (2001).
 - [13] K. Gross, C. P. Search, H. Pu, W. Zhang, and P. Meystre, Phys. Rev. A **66**, 033603 (2002).
 - [14] A. Einstein and W. J. de Haas, Verh. Dtsch. Phys. Ges. **17**, 152 (1915).
 - [15] S. J. Barnett, Phys. Rev. **6**, 239 (1915).
 - [16] T.-L. Ho, Phys. Rev. Lett. **81**, 742 (1998).
 - [17] J. Werner, A. Griesmaier, S. Hensler, J. Stuhler, T. Pfau, A. Simoni, and E. Tiesinga, Phys. Rev. Lett. **94**, 183201 (2005).
 - [18] After submission of our Letter, we become aware of a preprint by R. B. Diener and T.-L. Ho, cond-mat/0511751; our choice of $a_0 = 91$ corresponds to the C phase of this reference. We have also investigated the A and B phases in the same reference by taking other values of a_0 and found almost the same spin dynamics as that for $a_0 = 91$.
 - [19] M. R. Matthews, B. P. Anderson, P. C. Haljan, D. S. Hall, M. J. Holland, J. E. Williams, C. E. Wieman, and E. A. Cornell, Phys. Rev. Lett. **83**, 3358 (1999).
 - [20] A. E. Leanhardt, Y. Shin, D. Kielpinski, D. E. Pritchard, and W. Ketterle, Phys. Rev. Lett. **90**, 140403 (2003).
 - [21] L. Santos and T. Pfau, cond-mat/0510634.